

FIG. 1: A graphical comparison of the standard and proposed electron EDM search methods. (a) The standard spin interferometer (SI) method is shown on a Bloch sphere for the stretched spin states in the presence of static electric and magnetic fields. The P, T -violating Hamiltonian is diagonal in this subspace, and leads to an extra phase $\omega_{PT}\tau$ in addition to that from the static magnetic field. (b) The clock transition (CT) method is shown on a Bloch sphere for the two clock states in the presence of oscillating electric and magnetic fields. The P, T -violating Hamiltonian is off-diagonal in this subspace, and leads to an extra transition amplitude $\Omega_{PT}\tau$ in addition to the amplitude due to that from the oscillating magnetic field.

The molecule polarizes in the electric field, leading to a nonzero expectation value for the orientation $\zeta = \langle \hat{n} \cdot \hat{z} \rangle$ ($\langle \hat{n} \cdot \hat{x} \rangle = \langle \hat{n} \cdot \hat{y} \rangle = 0$ due to azimuthal symmetry). The interaction Hamiltonian for just the electron and nuclear spin degrees of freedom is then

$$H_{\text{int}} = -(g_s S_z + g_I I_z) \mu_B \mathcal{B}_z + W_{PT} S_z \zeta. \quad (2)$$

The molecular orientation $\zeta = \langle \hat{n} \cdot \hat{z} \rangle$ depends on the applied electric field \mathcal{E}_z , the dipole moment D , and the energy separation between opposite parity states in the molecule [see Supplementary Material (SM), Sec. A].

The standard electron EDM search method measures the energy difference between the stretched hyperfine states $|F = 1, m_F = \pm 1\rangle$ (see e.g., [22]). We denote these stretched hyperfine states as $|\uparrow\uparrow\rangle, |\downarrow\downarrow\rangle$. The energy difference between these states, $\omega_B + \omega_{PT} = -(g_s + g_I) \mu_B \mathcal{B}_z + W_{PT} \zeta$, is measured using a Ramsey-type technique which we will refer to as a spin interferometer (SI). The SI method is represented graphically in Fig. 1(a). First, the superposition state $|X\rangle = \frac{|\uparrow\uparrow\rangle + |\downarrow\downarrow\rangle}{\sqrt{2}}$ is prepared, starting from $|F = 0, m_F = 0\rangle$. Under the influence of the electric and magnetic fields for a time τ , the superposi-

tion evolves into the state $|\Psi\rangle = \frac{|\uparrow\uparrow\rangle + e^{i\phi} |\downarrow\downarrow\rangle}{\sqrt{2}}$. The phase $\phi = (\omega_B + \omega_{PT})\tau$ is extracted from $|\Psi\rangle$ by projectively measuring the populations in $|X\rangle$ and the orthogonal state $|Y\rangle = \frac{|\uparrow\uparrow\rangle - |\downarrow\downarrow\rangle}{\sqrt{2}}$. The P, T -violating phase $(\omega_{PT}\tau)$ is separated from the \mathcal{B} -dependent phase $(\omega_B\tau)$ by measuring ϕ under different combinations of the sign of the magnetic field \mathcal{B}_z and the molecular orientation ζ . The SI method, with some slight variations, is essentially used in every molecule-based electron EDM search experiment [3, 4, 18, 22, 24, 25].

Clock transition (CT) method. – Our proposed method uses time-dependent electric and magnetic fields to drive populations between the hyperfine clock states, $|g\rangle \equiv |F = 0, m_F = 0\rangle = \frac{|\uparrow\downarrow\rangle - |\downarrow\uparrow\rangle}{\sqrt{2}}$, and $|e\rangle \equiv |F = 1, m_F = 0\rangle = \frac{|\uparrow\downarrow\rangle + |\downarrow\uparrow\rangle}{\sqrt{2}}$. We consider time-dependent magnetic and electric fields applied to the molecules: $\mathcal{B}_z = \mathcal{B}_0 \cos(\omega_B t)$, $\mathcal{E}_z = \mathcal{E}_0 \cos(\omega_E t + \beta)$, where β is an adjustable phase. The oscillating electric field induces an oscillating molecular orientation with amplitude ζ_0 . The dependence of $\zeta = \langle \hat{n} \cdot \hat{z} \rangle$ on \mathcal{E}_z is nonlinear and so $\zeta(t)$ generally contains odd harmonics of ω_E as shown in Fig. 2 (see also Figs. 4, 5 in the SM). For now, let ζ_0 refer to the amplitude of oscillations at the fundamental frequency ω_E . We also assume for now that the electric and magnetic fields are driven at the same frequency, $\omega_E = \omega_B = \omega$.

We denote the energy separation between the clock states in the presence of $\mathcal{B}_z(t), \mathcal{E}_z(t)$ (i.e., including the zero-field hyperfine splitting, and the Zeeman and tensor Stark shifts) as ω_0 , and define the detuning $\Delta = \omega - \omega_0$. We make the rotating wave approximation for the time-dependent fields (assuming that the Bloch-Siegert shift from the counter-rotating term is also included in ω_0). Then the Hamiltonian from Eq. (2), in the two-dimensional subspace spanned by $|g\rangle$ and $|e\rangle$, is just

$$H_{\text{int}} = \frac{\Omega_B}{2} \sigma_x + \frac{\Omega_{PT}}{2} (\cos \beta \sigma_x + \sin \beta \sigma_y) + \frac{\Delta}{2} \sigma_z, \quad (3)$$

where $\sigma_{x,y,z}$ are Pauli matrices, and the Rabi frequencies for the Zeeman and P, T -violating interactions are $\Omega_B = -\frac{1}{2}(g_s + g_I) \mu_B \mathcal{B}_0$ and $\Omega_{PT} = \frac{1}{2} W_{PT} \zeta_0$ respectively.

We assume that the molecules are initially prepared in the ground hyperfine clock state $|g\rangle$. On resonance ($\Delta = 0$) and under the influence of H_{int} for a time τ , the population in the excited clock state $|e\rangle$ is $\rho_{ee}(\tau) = \sin^2 \left[\frac{(\Omega_B + \Omega_{PT} \cos \beta) \tau}{2} \right]$. (We have dropped terms that are quadratic in W_{PT} .) The P, T -violating signal is contained in the frequency of the Rabi oscillations of the clock state populations. The measurement of W_{PT} from the population ρ_{ee} (or $\rho_{gg} = 1 - \rho_{ee}$) is illustrated in Fig. 3. The magnetic field amplitude \mathcal{B}_0 and the pulse duration τ are set so that $\Omega_B \tau \approx \pm \frac{\pi}{2}$ (modulo 2π), and the populations of the clock states are measured for different phase angles β . When $\beta = 0$ ($\beta = \pi$) the P, T -violating term Ω_{PT}

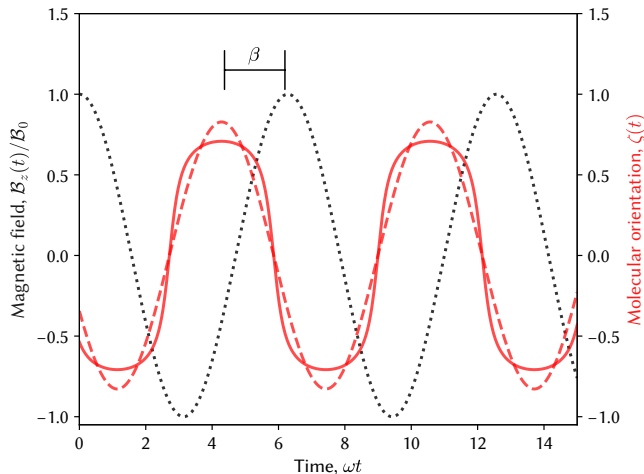


FIG. 2: The magnetic field $\mathcal{B}_z(t)$ (black, dots) and molecular orientation $\zeta(t)$ (red, solid) in the CT method. The curve for $\zeta(t)$ is the calculated molecular response to an electric field $\mathcal{E}_z(t) = \mathcal{E}_0 \cos(\omega t + \beta)$ (see SM, Sec. A). The red dashed line shows the first harmonic of ω in $\zeta(t)$.

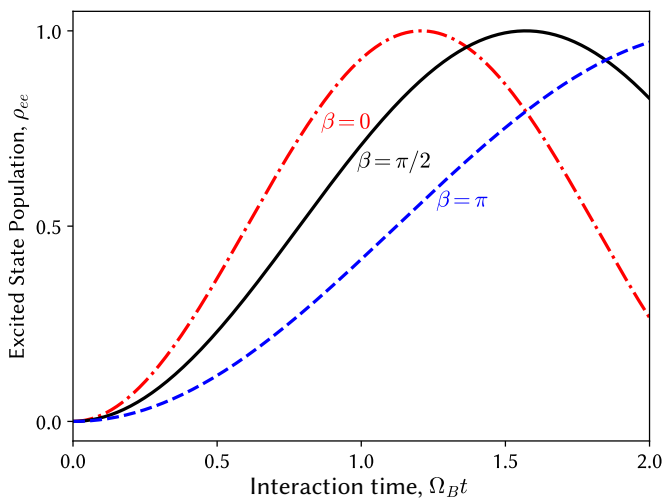


FIG. 3: The population in the excited clock state $|e\rangle = \frac{|\uparrow\downarrow\rangle + |\downarrow\uparrow\rangle}{\sqrt{2}}$ as a function of time, with the electric and magnetic fields driven at resonance (Ω_{PT} is greatly exaggerated for illustration). The relative phase β between $\mathcal{E}_z(t)$ and $\mathcal{B}_z(t)$ can be varied to separate the small P, T -violating contribution to the Rabi frequency from the larger magnetic-field-induced Rabi frequency.

adds to (subtracts from) Ω_B , leading to an increase (decrease) in ρ_{ee} . Setting $\beta = \pm\pi/2$ leaves ρ_{ee} unchanged, and offers a convenient null test. With an ensemble of N uncorrelated molecules subjected to H_{int} for a time τ , the precision achievable in a projection-noise-limited measurement of W_{PT} is $\delta W_{PT} = \frac{2}{\zeta_0 \tau \sqrt{N}}$. For YbF for example, a measurement with precision $\delta W_{PT} = 2\pi \times 10^{-6}$

Hz leads to an electron EDM uncertainty $\delta d_e = 10^{-31} e$ cm [22, 26].

We have discussed electron EDM searches using molecules with $^2\Sigma$ ground states so far, but the CT method is also applicable to nuclear EDM searches using $^1\Sigma$ diatomic molecules with $m_F = 0$ hyperfine states (e.g., $^{207}\text{Pb}^{17}\text{O}$). The hyperfine splitting ω_0 in such molecules arises from dipolar coupling of the two nuclei, and is consequently smaller (typically $\omega_0 \sim 2\pi \times 10$ kHz). For nuclear EDM searches, the quantities \vec{S} and S_z in Equations (1) and (2) are to be replaced by \vec{I}_M and $I_{M,z}$ respectively, where I_M is the spin of the P, T -violation-sensitive nucleus (^{207}Pb in our example). The quantity W_{PT} is to be understood as the expectation value of the nuclear EDM (arising from P, T -violating nuclear interactions and quark EDMs) interacting with the electric field inside a fully oriented molecule. The remainder of our discussion is also applicable to nuclear EDM searches.

Advantages. – Viewed on the Bloch sphere (Fig. 1), it is evident that the CT method is a “rotated” version of the usual SI method. It is therefore unsurprising that the CT and SI methods have comparable statistical sensitivities. However, there are some practical advantages to the CT method:

- The frequency ω_0 (and thus Δ) is insensitive to magnetic fields to first order, and the Rabi fringe phase is further only quadratically sensitive to Δ when $\Delta \lesssim \Omega_B$. Therefore the requirements for shielding low-frequency stray magnetic fields are severely relaxed. Polar molecules with special internal structure (e.g., Ω -doublets or ℓ -doublets) to track and cancel magnetic field drifts are no longer required. This allows ground-state polar molecules with simple electronic structure (e.g., $^2\Sigma$ or $^1\Sigma$) to be used in competitive electron or nuclear EDM experiments.
- The coherence times for hyperfine state superpositions, which are insensitive to magnetic noise, are much longer than coherence times for stretched state superpositions. This allows large values of τ to be practically realized, leading to improved statistical sensitivity.
- The initial state preparation in this method is simple: it is easy to accurately initialize molecules in the ground hyperfine state, compared to preparing an accurate superposition $|X\rangle$ in the SI method. This feature can improve the duty cycle of experiments and eliminate systematics that arise from imperfect state preparation.
- Just as stray static magnetic fields lead to spurious phase accumulation in the SI method, stray radio-frequency (rf) magnetic fields in the neighborhood of $\omega_0 \pm 1/\tau$ can shift the Rabi frequency in the

CT method. However, shielding rf magnetic fields is significantly easier than shielding low-frequency magnetic fields.

- e) The phase β between the electric and magnetic fields can be varied rapidly and smoothly, without correlated switching transients and charging currents that usually accompany reversals of DC electric fields. This allows potential systematics (e.g., from drifts in Ω_B or non-reversing electric fields) to be cleanly cancelled.
- f) This method can be applied to molecular ions, since the hyperfine resonance frequency ω_0 can be chosen to be far away from typical ion trap motional frequencies. Therefore the method enables EDM experiments with a wide class of molecular ions without imposing further constraints, such as requiring ${}^3\Delta_1$ molecular structure, for the sake of magnetic field control. In particular, this opens a feasible approach to EDM searches using nuclei that are short-lived but highly sensitive to P, T -violation (e.g., ${}^{225}\text{Ra}$ [27], ${}^{229}\text{Pa}$ [28], ${}^{285}\text{Cn}$ [29]), where there may only be limited options for molecules that can be efficiently created from rare isotope sources.

Controlling systematics. – A genuine W_{PT} -dependent signal can be identified as the part of ρ_{ee} that changes sign under switches of (i) the initial state ($|e\rangle$ or $|g\rangle$), (ii) the phase β (0 or π), and (iii) the pulse area Ω_{BT} ($\pm\pi/2$ modulo 2π), allowing \mathcal{B}_z and τ to be varied over a large dynamic range to find systematic errors. The P, T -violating observable in the CT method is an off-diagonal matrix element or Rabi frequency, rather than an energy shift as in the SI method. Therefore transition amplitudes that are in phase with the driving electric field can lead to systematic errors.

One strategy for detecting such errors, just as in SI experiments, is to make measurements in states (e.g., $m_F = 0 \rightarrow m_F = 0$ transitions in the $N = 0$ and $N = 1$ rotational manifolds) that have similar responses to magnetic fields but different magnitudes and signs of ζ . Such states can function as adequate internal co-magnetometers even in simple ${}^2\Sigma$ molecules (see e.g., [30]). However a new source of potential systematic errors in the CT method is the displacement current due to the oscillating \mathcal{E} -field. This induces a \mathcal{B} -field with amplitude $\mathcal{B}_d \sim \frac{\ell\omega_E}{c^2}\mathcal{E}_0$, where ℓ is a length scale on the order of the size of the electrodes. With $\ell \sim 1$ cm, $\mathcal{E}_0 \sim 10$ kV/cm and $\omega_E = 2\pi \times 10$ MHz, the displacement \mathcal{B} -field has amplitude $\mathcal{B}_d \sim 50$ mG, which leads to a spurious Rabi frequency $\Omega_d \sim 2\pi \times 100$ kHz that mimics Ω_{PT} . We describe a way to suppress this effect. First, the displacement \mathcal{B} -field is perpendicular to $\vec{\mathcal{E}}$, which suppresses shifts in ρ_{ee} because \mathcal{B} -fields in the xy -plane only couple $|F = 0, m_F = 0\rangle$ to the $|F' = 1, m_{F'} = \pm 1\rangle$ levels. Further, these transitions are out of resonance with the frequency $\omega_E = \omega_0$ due to

the tensor Stark shift in polar molecules [26, 31, 32]. Any residual \mathcal{B} -field component along \hat{z} , due to mis-alignment of the electrodes for example, can be further suppressed using the fact that the induced \mathcal{B} -field is proportional to the time derivative of \mathcal{E}_z , and therefore lags the applied \mathcal{E} -field in phase by $\pi/2$. For example, if $\vec{\mathcal{B}}_d \cdot \hat{z} \neq 0$ and β is set to $\pm\pi/2$, there will be a change in ρ_{ee} depending on whether the \mathcal{E} -field is on or off. Such a shift is only produced when $\vec{\mathcal{B}}_d \cdot \hat{z} \neq 0$, and can therefore be used as a diagnostic for displacement \mathcal{B} -fields. Despite these, it is conceivable that a combination of phase errors (due to charging currents or cable impedance mismatches) and electrode imperfections could still lead to a residual \mathcal{B} -field that is both parallel to \hat{z} and in phase with \mathcal{E}_z : misalignment of the rf electric and magnetic field directions by $\theta = 0.1$ mrad, and a phase error in the electric field drive by $\Delta\beta = 1$ mrad would lead to a residual Rabi frequency $\Omega'_d = \theta \Delta\beta \Omega_d = 2\pi \times 10$ mHz that mimics Ω_{PT} .

We point out that there is a general way to further suppress systematic errors generated by the oscillating \mathcal{E} -field, using the fact that the molecular orientation ζ is nonlinear in \mathcal{E}_z . If \mathcal{E}_0 is large enough to appreciably polarize the molecule, then $\zeta(t)$ also contains higher odd harmonics of ω_E (see SM, Fig. 5). Therefore, an EDM search experiment can be conducted using, e.g., $\omega_E = \omega_0/3$ and $\omega_B = \omega_0$. Any induced magnetic fields that are linear in \mathcal{E}_z (a condition which covers the majority of conceivable systematics) oscillate at $\omega_0/3$, far off resonance from the clock transition, and so their interference with the transition amplitude is greatly suppressed. On the other hand, the fourier component of ζ that oscillates at $3\omega_E = \omega_0$ (with amplitude ζ_3) resonantly contributes to the transition probability as $\rho_{ee}(\tau) = \sin^2 \left[\frac{(\Omega_B + \Omega_{PT,3} \cos 3\beta) \tau}{2} \right]$, with $\Omega_{PT,3} = \frac{1}{2} W_{PT} \zeta_3$. Therefore, driving the electric field at a sub-harmonic of ω_0 offers a convenient diagnostic for discriminating between systematic errors and real P, T -violating signals. Since $\zeta_3 < \zeta_0$ though, it yields lower EDM sensitivity, so we envision that experiments using the CT method will intersperse some measurements with $\omega_E = \omega_0/3$ as systematic checks within larger measurement blocks with $\omega_E = \omega_0$.

We have also considered systematic errors due to effects such as $E1 - M1$ mixing: static background electric (\mathcal{E}_{dc}) and magnetic (\mathcal{B}_{dc}) fields can admix states in the $N = 0$ and $N = 1$ manifolds. This induces a transition Rabi frequency $\Omega_{E1-M1} \propto \mathcal{E}_{dc} \mathcal{B}_{dc} \mathcal{E}_0$ driven by $\mathcal{E}_z(t)$ which mimics Ω_{PT} . Numerical and perturbative calculations for the parameters of YbF (see SM, Sec. A), using realistic estimates of the background fields $\mathcal{E}_{dc} = 1$ V/cm and $\mathcal{B}_{dc} = 10$ mG, yield $\Omega_{E1-M1} \sim 2\pi \times 10^{-10}$ Hz, which is a negligible systematic error compared to the expected precision of electron EDM experiments with trapped molecules.

In summary, we have devised a measurement technique using hyperfine clock states that offers advantages for

electric dipole moment searches using polar molecules. The use of magnetically insensitive states enables longer coherence times for improved precision, and leads to an enhanced level of systematic error control. Our method opens up a wide selection of polar molecules for use in high-precision EDM search experiments – in particular, this includes simple diatomic molecules that can be directly laser-cooled or assembled out of ultracold atoms.

We thank Wes Campbell, Jonathan Weinstein and David DeMille for helpful comments. M.V. acknowledges support from NSERC and an Ontario Graduate Scholarship. A.M.J. acknowledges support from NSF Grant No. PHY-1912665. A.C.V. acknowledges support from Canada Research Chairs and a Sloan Fellowship.

* vutha@physics.utoronto.ca

- [1] D. DeMille, J. M. Doyle, and A. O. Sushkov, *Science* **357**, 990 (2017).
- [2] M. S. Safronova, D. Budker, D. DeMille, D. F. J. Kimball, A. Derevianko, and C. W. Clark, *Rev. Mod. Phys.* **90**, 025008 (2018).
- [3] W. B. Cairncross, D. N. Gresh, M. Grau, K. C. Cossel, T. S. Roussy, Y. Ni, Y. Zhou, J. Ye, and E. A. Cornell, *Phys. Rev. Lett.* **119**, 153001 (2017).
- [4] ACME Collaboration: V. Andreev *et al.*, *Nature* **562**, 355 (2018).
- [5] J. L. Feng, *Annu. Rev. Nucl. Part. Sci.* **63**, 351 (2013).
- [6] D. Cho, K. Sangster, and E. A. Hinds, *Phys. Rev. Lett.* **63**, 2559 (1989).
- [7] E. Norrgard, D. McCarron, M. Steinecker, M. Tarbutt, and D. DeMille, *Phys. Rev. Lett.* **116**, 063004 (2016).
- [8] S. Truppe, H. Williams, M. Hambach, L. Caldwell, N. Fitch, E. Hinds, B. Sauer, and M. Tarbutt, *Nat. Phys.* **13**, 1173 (2017).
- [9] A. L. Collopy, S. Ding, Y. Wu, I. A. Finneran, L. Anderegg, B. L. Augenbraun, J. M. Doyle, and J. Ye, *Phys. Rev. Lett.* **121**, 213201 (2018).
- [10] L. W. Cheuk, L. Anderegg, B. L. Augenbraun, Y. Bao, S. Burchesky, W. Ketterle, and J. M. Doyle, *Phys. Rev. Lett.* **121**, 083201 (2018).
- [11] M. Guo, B. Zhu, B. Lu, X. Ye, F. Wang, R. Vexiau, N. Bouloufa-Maafa, G. Quéméner, O. Dulieu, and D. Wang, *Phys. Rev. Lett.* **116**, 205303 (2016).
- [12] T. M. Rvachov, H. Son, A. T. Sommer, S. Ebadi, J. J. Park, M. W. Zwierlein, W. Ketterle, and A. O. Jamison, *Phys. Rev. Lett.* **119**, 143001 (2017).
- [13] L. De Marco, G. Valtolina, K. Matsuda, W. G. Tobias, J. P. Covey, and J. Ye, *Science* **363**, 853 (2019).
- [14] A. Sunaga, V. S. Prasanna, M. Abe, M. Hada, and B. P. Das, *Phys. Rev. A* **99**, 040501 (2019).
- [15] J. Lim, J. R. Almond, M. A. Trigatzis, J. A. Devlin, N. J. Fitch, B. E. Sauer, M. R. Tarbutt, and E. A. Hinds, *Phys. Rev. Lett.* **120**, 123201 (2018).
- [16] T. Fleig and D. DeMille, private communication (2019).
- [17] E. B. Norrgard, E. R. Edwards, D. J. McCarron, M. H. Steinecker, D. DeMille, S. S. Alam, S. K. Peck, N. S. Wadia, and L. R. Hunter, *Phys. Rev. A* **95**, 062506 (2017).
- [18] I. Kozyryev and N. R. Hutzler, *Phys. Rev. Lett.* **119**, 133002 (2017).
- [19] D. DeMille *et al.*, in *Art and Symmetry in Experimental Physics (AIP Conf. Proc. 569)* (2001) pp. 72–83.
- [20] E. R. Meyer and J. L. Bohn, *Phys. Rev. A* **80**, 042508 (2009).
- [21] A. E. Leanhardt, J. L. Bohn, H. Loh, P. Maletinsky, E. R. Meyer, L. C. Sinclair, R. P. Stutz, and E. A. Cornell, *J. Mol. Spec.* **270**, 1 (2011).
- [22] J. J. Hudson, D. M. Kara, I. Smallman, B. E. Sauer, M. R. Tarbutt, and E. A. Hinds, *Nature* **473**, 493 (2011).
- [23] E. D. Commins, in *Advances in Atomic, Molecular, and Optical Physics*, Vol. 40 (Elsevier, 1999) pp. 1–55.
- [24] NL-eEDM collaboration: P. Aggarwal *et al.*, *Eur. Phys. J. D* **72**, 197 (2018).
- [25] A. C. Vutha, M. Horbatsch, and E. A. Hessels, *Phys. Rev. A* **98**, 032513 (2018).
- [26] J. J. Hudson, B. E. Sauer, M. R. Tarbutt, and E. A. Hinds, *Phys. Rev. Lett.* **89**, 023003 (2002).
- [27] M. Bishof, R. H. Parker, K. G. Bailey, J. P. Greene, R. J. Holt, M. R. Kalita, W. Korsch, N. D. Lemke, Z.-T. Lu, P. Mueller, T. P. O’Connor, J. T. Singh, and M. R. Dietrich, *Phys. Rev. C* **94**, 025501 (2016).
- [28] J. T. Singh, *Hyperfine Interactions* **240**, 29 (2019).
- [29] L. Radžiūtė, G. Gaigalas, P. Jönsson, and J. Bieroń, *Phys. Rev. A* **93**, 062508 (2016).
- [30] V. S. Prasanna, A. C. Vutha, M. Abe, and B. P. Das, *Phys. Rev. Lett.* **114**, 183001 (2015).
- [31] I. B. Khriplovich and S. K. Lamoreaux, *CP violation without strangeness: electric dipole moments of particles, atoms, and molecules* (Springer-Verlag, Berlin, 1997).
- [32] D. DeMille, F. Bay, S. Bickman, D. Kawall, D. Krause, S. E. Maxwell, and L. R. Hunter, *Phys. Rev. A* **61**, 052507 (2000).
- [33] B. Sauer, J. Wang, and E. Hinds, *J. Chem. Phys.* **105**, 7412 (1996).
- [34] T. A. Isaev, S. Hoekstra, and R. Berger, *Phys. Rev. A* **82**, 052521 (2010).
- [35] M. Abe, private communication (2018).

SUPPLEMENTARY MATERIAL

A. Calculation of the molecular orientation

The field-free Hamiltonian for the $^2\Sigma$ electronic ground state of a molecule such as $^{174}\text{Yb}^{19}\text{F}$ is

$$H_0 = B_{\text{rot}}N(N+1) + \gamma\vec{S}\cdot\vec{N} + b\vec{S}\cdot\vec{I} + cS_zI_z, \quad (4)$$

where \vec{N} , \vec{S} , \vec{I} are the molecular rotational angular momentum, electron spin and nuclear spin respectively. B_{rot} is the rotational constant of the molecule, γ is the spin-rotation parameter, and b, c are hyperfine interaction parameters. In an electric field, the interaction Hamiltonian (see Eq. (1)) is $H_{\text{int}} = D\hat{n}\cdot\vec{\mathcal{E}}$ where D is the molecular dipole moment. A characteristic scale for the electric field required to polarize the molecule can be constructed from these constants, $\mathcal{E}_{\text{pol}} = 2B_{\text{rot}}/D$.

We used the uncoupled computational basis $|N, m_N; S, m_S; I, m_I\rangle$, including rotational levels up to $N = 20$, and numerically diagonalized $H_0 + H_{\text{int}}$ for different values of \mathcal{E}_z . The resulting dependence of the molecular orientation $\zeta = \langle\hat{n}\cdot\hat{z}\rangle$ is shown in Fig. 4. For this calculation, we used measured values of $B_{\text{rot}}, \gamma, b, c$ for $^{174}\text{Yb}^{19}\text{F}$ [33] – the resulting value of $\mathcal{E}_{\text{pol}} = 7.3$ kV/cm. (This value of \mathcal{E}_{pol} lies near the higher end for the list of molecules in Section B.) When the curve of ζ versus \mathcal{E}_z is smoothly interpolated and applied to a sinusoidal electric field $\mathcal{E}_z(t) = \mathcal{E}_0 \cos(\omega t + \beta)$ (with $\mathcal{E}_0 = 3\mathcal{E}_{\text{pol}}$), the curve for $\zeta(t)$ in Fig. 2 is obtained.

We also use this numerical model to calculate systematic errors, such as the $E1 - M1$ mixing-induced Rabi frequency Ω_{E1-M1} described in the main text. The numerical calculations confirm the estimate from perturbation theory, $\Omega_{E1-M1} \sim D\mathcal{E}_0 (D\mathcal{E}_{\text{dc}}) (g_S\mu_B\mathcal{B}_{\text{dc}}) \frac{\gamma^2}{B_{\text{rot}}^4}$.

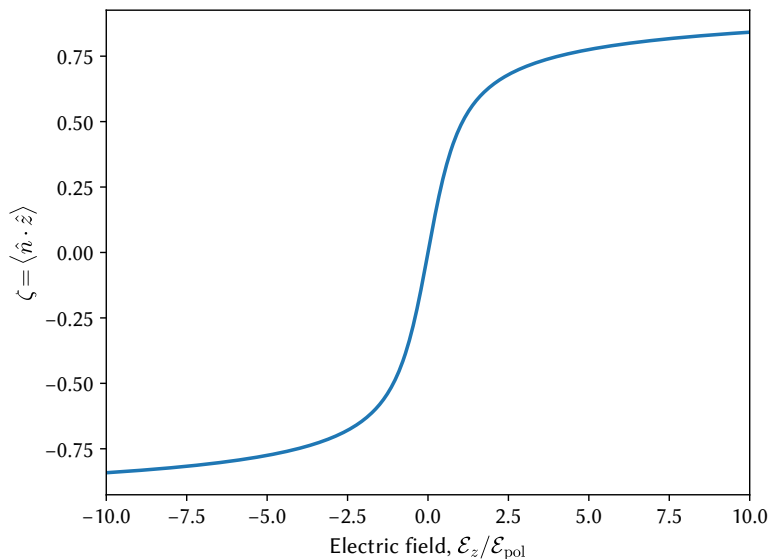


FIG. 4: Molecular orientation $\zeta = \langle\hat{n}\cdot\hat{z}\rangle$ as a function of the electric field applied to the molecule.

B. Molecules for electron and nuclear EDM searches

The following tables list neutral molecules (Table I) and singly-charged molecular ions (Table II) that can be used for electron EDM and nuclear EDM searches using the CT method. In each table, a combination of species from the two columns forms an EDM-sensitive molecule to which the CT method can be applied. The tables are by no means exhaustive – other analogous molecular systems can potentially be used. The tables include some molecules that have been previously used (YbF [22]) or proposed for use in EDM experiments (HgF, HgCl, HgBr [30], HgNa, HgK, HgRb [14], RaF [34], BaF [24], RaAg [16], HgCa [35]). The CT method can also be applied to other molecules that do not fall into the tables' categories (e.g., $^{205}\text{Tl}^{19}\text{F}$).

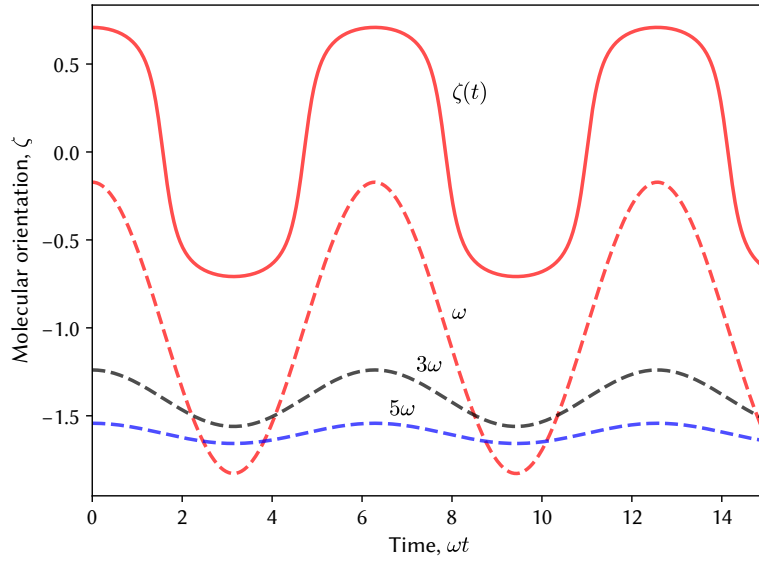


FIG. 5: Molecular orientation $\zeta = \langle \hat{n} \cdot \hat{z} \rangle$ in response to an electric field $\mathcal{E}_z(t) = 3\mathcal{E}_{\text{pol}} \cos \omega t$. The harmonics contained in $\zeta(t)$ are offset for clarity.

TABLE I: Neutral molecules.

Electron EDM

^{138}Ba	^{19}F
^{174}Yb	^{35}Cl
^{202}Hg	^{79}Br
^{226}Ra	^{107}Ag
	$^{16}\text{O}^1\text{H}$

Nuclear EDM

^{199}Hg	^{17}O
^{207}Pb	^{33}S
^{225}Ra	^{43}Ca
	^{87}Sr

TABLE II: Molecular ions.

Electron EDM

^{200}Hg	^{17}O
^{226}Ra	^{33}S
^{208}Pb	^{43}Ca
^{232}Th	^{87}Sr

Nuclear EDM

^{133}Ba	^{19}F
^{199}Hg	^{35}Cl
^{207}Pb	^{79}Br
^{225}Ra	$^{16}\text{O}^1\text{H}$
^{229}Pa	
^{229}Th	